

Latent heat estimation with machine learning

Diana Sukhoverkhova^{1,2}, Vyacheslav Mozolenko^{1,2}, and Lev Shchur^{1,2}
¹ Landau Institute for Theoretical Physics, 142432 Chernogolovka, Russia and
² HSE University, 101000 Moscow, Russia

We set out to explore the possibility of investigating the critical behavior of systems with first-order phase transition using deep machine learning. We propose a machine learning protocol with ternary classification of instantaneous spin configurations using known values of disordered phase energy and ordered phase energy. The trained neural network is used to predict whether a given sample belong to one or the other phase of matter. This allows us to estimate the probability that configurations with a certain energy belong to the ordered phase, mixed phase, and disordered phase. From these probabilities, we obtained estimates of the values of the critical energies and the latent heat for the Potts model with 10 and 20 components, which undergoes a strong discontinuous transition. We also find that the probabilities can reflect geometric transitions in the mixed phase.

Introduction. — The application of deep neural networks for supervised machine learning [1] to study the critical behavior of models with second-order phase transition allows us to estimate the critical temperature [2, 3] and the critical exponent of the correlation length [4]. Examples include the study of Ising model, the Baxter-Wu model, the Potts model and the XY model, and percolation problem and many others [3–10]. The approach proved to be quite robust also in the study of the Ising model with non-trivial diagonal anisotropy [11] and in cross-training between universality classes [12]. This approach is based on binary classification of Monte Carlo-generated instantaneous configurations of the model into ferromagnetic and paramagnetic phases during training and the application of a trained neural network to predict whether the tested instantaneous configurations generated at a known temperature belong to one of these two phases. In this way, the probability distribution in sample space at temperature T of belonging to the ferromagnetic or paramagnetic phase is estimated. Finite-size analysis of this function and its variation allows us to estimate with satisfactory accuracy the critical temperature and the exponent of the critical correlation length [3, 4].

In the case of phase transitions of the first kind, the phase transition temperature can also be estimated by a learning/testing approach similar to the one mentioned above, using learning relative to a known critical temperature. However, with this approach, it is not possible to estimate the values of the critical energies and hence the magnitude of the latent heat, i.e., the difference between the energies of the ordered e_o and disordered e_d phases at the phase transition temperature. A neural network trained on binary classification cannot capture the mixed phase, which is a hallmark of systems with phase transition of the first kind. A different approach is required. In this letter, we propose a new method for solving such a problem.

The method is based on supervised learning, but instead of binary classification, a ternary classification of instantaneous spin configurations is used. The classification is performed relative to known critical values of

energies e_o and e_d : OS - ordered phase for samples with energy $e < e_o$, MS - mixed phase for samples with energy $e_o < e < e_d$, DS - disordered phase for samples with energy $e > e_d$ [13]. In the testing phase, a snapshot of the spin configuration obtained at a certain energy e is fed to the input of the neural network, and the network produces three numbers corresponding to predictions that the tested configuration with energy e may belong to one of the three phases. Based on testing a large number of configurations at the same value of energy e , we obtain an estimate of the probability that the tested snapshots with energy e belong to one of the three phases.

The application of such a method requires a large number of uncorrelated sample data sets with a certain energy value for training and testing the neural network. Modeling such datasets usually takes a large amount of time [14, 15]. Fortunately, a microcanonical population annealing (MCPA) [16, 17] algorithm has recently been developed that generates a large number of replicas of the system under study using parallel acceleration on GPUs and filters a fraction of the replicas at a given energy [16, 17]. We simulated 2^{17} replicas for the Potts model with 10 and 20 components [18]. Detailed analysis showed good qualities of the method both in comparison with another microcanonical Wang-Landau method and with known exact results [19]. In the simulation, at each step of the algorithm, we randomly selected at each energy value $2^{13} = 8192$ replicas from the current replica pool and used them for training the neural network and for testing and analysis. The density of states in the neighborhood of critical energies is a decreasing function of energy, and when applying the MCPA ceiling algorithm step with decreasing energy [16] most of the population of 2^{17} configurations will be concentrated near the energy ceiling. Furthermore, all replicas are randomly “equilibrated” on a lattice of size $L \times L$ with an MCMC step number of $10L^2$. Thus, it is hoped that there are no observable correlations between configurations in the chosen small fraction of replicas. Indeed, our results support this assumption.

Model. — We consider the Potts model on a square

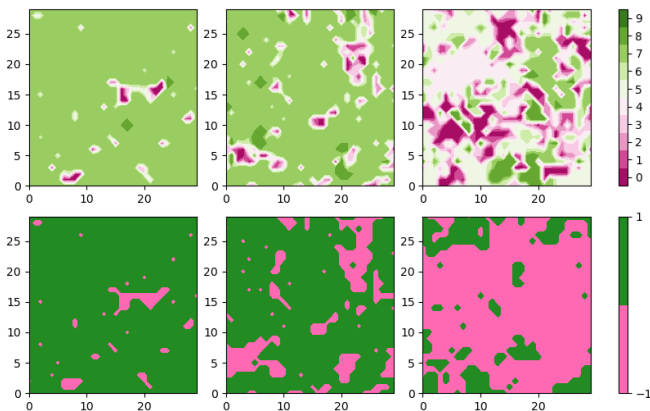


FIG. 1. Typical spin configurations for the 10-state Potts model on the $L = 30$ lattice at energies from left to right: $e = -1.9$ in the ordered phase, $e = -1.4$ in the mixed state, and $e = -0.9$ in the disordered state. The upper panel is the raw RD dataset RD and lower panel is the majority/minority MD dataset.

lattice $L \times L$ with periodic boundaries; spins $s_i \in \{0, \dots, q-1\}$; summation over all pairs of spins (s_i, s_j) with Hamiltonian $H = -\sum_{\langle i,j \rangle} \delta_{s_i, s_j}$. The critical values of the ordered and disordered phases are known exactly [18] and values are $e_o \approx -1.664252$ and $e_d \approx -0.968203$ for 10-state Potts model and $e_o \approx -1.820684$ and $e_d \approx -0.626529$ for 20-state Potts model. Hereafter, we will refer to these models as PM-10 and PM-20 for short.

Sample generation. — The MCPA method [16, 17] is used to obtain samples. Details and performance of the algorithm in the application to the Potts model with 10 and 20 states can be found in the paper [19]. At each energy value, the 8192 configurations are divided in a 3:1 ratio, i.e., 6144 spin configurations are used for training and 2048 configurations are used for predictions and probability estimation. The energy of the samples varied in the range $-2 < e < -0.5$.

Data preprocessing. — Typical PM-10 configurations corresponding to ordered, mixed and disordered states are shown in the figure 1, the color scale on the right corresponds to the instantaneous spin values. There are two ways to represent spin configuration for Potts model, which we marked with the abbreviations: RD - the raw data and MD - in each configuration the spins belonging to the largest component m in $q = 0, 1, \dots, q-1$ is marked as +1 and the rest of spins with the -1. The second line of figure 1 illustrates the result of the top line with raw RD configurations mapped to majority/minority MD configurations in all three phase states. This representation is inspired by the way the magnetisation is calculated in the Potts [20] model with spin m majority by $M = (qN_m/L^2 - 1)/(q - 1)$, where N_m is the number of sites i with $s_i = m$. The dependence of magnetization of average magnetization $\langle m \rangle$, calculated over all configurations

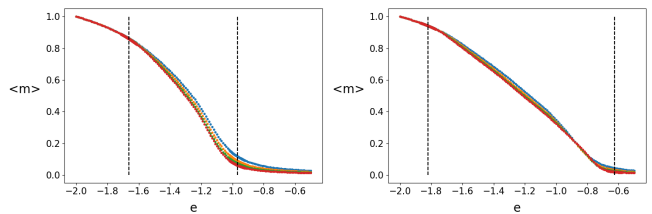


FIG. 2. Magnetization $\langle m \rangle$ for lattice sizes $L = 30, 40, 50$ and for two models calculated with RD datasets: left panel with PM-10 and right panel with PM-20.

with energy e , is plotted in Figure 2 for several values of L and for two models, PM-10 and PM-20. In Figure 1, the green color in the bottom panel reflects majority spins, which corresponds to $m = 7$ in the left and middle pictures of the top panel, and $m = 5$ in the right picture.

Training. — We use CNN neural network [21] with binary cross-entropy loss function and Adam optimization algorithm [22] with parameters $\alpha = 10^{-3}$, $\beta_1 = 0.9$, $\beta_2 = 0.999$, $\varepsilon = 10^{-8}$. The NN(L) network is trained for each lattice size L and each RD and MD dataset separately. The spin configuration labelled as OS, MS or DS is fed to the NN for ternary classification training into ordered, mixed and disordered states. The network is trained in one epoch [23]. The total number of configurations used in training $NN(L)$ is several million.

Predictions and phase probabilities. — The remaining 25% of the samples are used for predictions. Each configuration i of size $L \times L$ sampled in MCPA simulations with energy e is fed to the input of a trained network NN(L). The network outputs three numbers predicting membership of the ordered phase $p_{OS}^i(e)$, mixed phase $p_{MS}^i(e)$, and disordered phase $p_{DS}^i(e)$. The sum of these three numbers is equal to one. We repeat this process over the sample space, containing $N_{test} = 2048$ samples with the given energy e . We calculated estimates of the probabilities $P_{xS}(e)$ averaging predictions $p_{xS}^i(e)$ over the sample space, $P_{xS}(e) = \sum_{i=1}^{N_{test}} p_{xS}^i(e)/N_{test}$, where xS stands for one of the three phases, OS, MS, or DS. Thus, we obtain the probability functions $P_{OS}(e)$, $P_{MS}(e)$, and $P_{DS}(e)$, with $P_{OS}(e) + P_{MS}(e) + P_{DS}(e) = 1$. Figures 3 and 4 show an example of phase probability estimation for model PM-10 and model PM-20, respectively, and present the results for both datasets, RD and MD. The network correctly predicts the phases of the models, and the smoothed sharp change in the probabilities near critical energies is explained by the finiteness of the system under study. The physics of some of the details is discussed in the last section “Discussion”.

Energy and latent heat estimations. — To estimate the energy of the ordered phase e_o , we chose several (in fact we stopped at seven) points belonging to each set

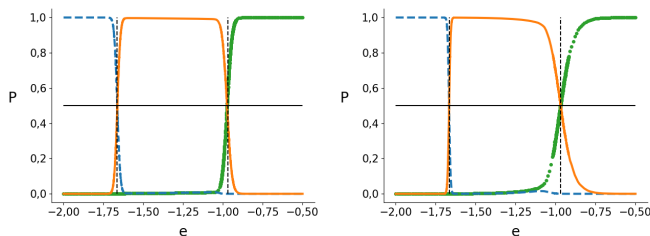


FIG. 3. Probabilities of phases $P_x S(E)$ for $L = 60$ for 10-state Potts model, PM-10. Left panel is the training/testing with the raw dataset RD and right panel is the training/testing with the majority/minority dataset MD.

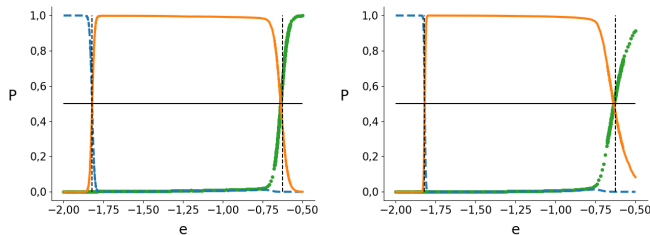


FIG. 4. Probabilities of phases $P_x(E)$ for $L = 60$ for 20-state Potts model, PM-20. Left panel is the training/testing with the raw dataset RD and right panel is the training/testing with the majority/minority dataset MD.

$P_{OS}(e)$ and $P_{MS}(e)$ in the neighborhood of their intersection, and approximated these points by two straight lines, respectively. The intersection of these straight lines gives an estimate of e_o . Similarly, the estimate for e_d is obtained from the sets $P_{MS}(e)$ and $P_{DS}(e)$. The resulting estimates are presented in the tables.

Tables I and II present estimates of critical energies e_o and e_d and latent heat for the 10-component Potts model, PM-10. Each row of critical energy estimates is followed by a row with the ratio of the deviation of the estimated critical energy to the statistical error to show the quality of the estimate. We find no noticeable finite-size corrections.

In the case of a continuous transition driven by thermodynamic fluctuations, we see that finite-size analysis of machine learning probabilities reflects these fluctuations and leads to a reasonable estimate of the critical length exponent [3, 4]. In the case of a discontinuous phase transition, the correlation length does not diverge, and the dependence on the finite size may be different. It is known that finite-size corrections to thermodynamic quantities in the Potts model are very sensitive to the way they are estimated and depend on the quantities of interest. In two-dimensional space, the corrections can be proportional to $1/L$ or $1/L^2$ or even $1/L^4$ [19, 24–26].

The phase prediction probability of a neural network is not a thermodynamic function, but at the same time its fluctuations can somehow reflect thermodynamic fluctua-

tions, which may lead to the visible finite-size corrections. The correlation length is finite and approximately equal to 10.6 for the PM-10 model [24]. Interestingly, even moderate sizes of the studied systems compared to the correlation length allow us to estimate the critical values of the energies, and through them the latent heat, with an accuracy not worse than few percent.

L	30	40	50	60	Exact
e_o	-1.650(20)	-1.667(6)	-1.667(6)	-1.663(6)	-1.66425...
$\frac{\Delta e_o}{\sigma_o}$	0.7	0.5	0.5	0.2	
e_d	-0.952(28)	-0.977(1)	-0.954(5)	-0.974(1)	-0.96820...
$\frac{\Delta e_d}{\sigma_d}$	0.6	8.8	2.8	5.8	
\mathcal{L}	0.698(48)	0.690(7)	0.713(11)	0.689(7)	0.696049...
$\Delta\mathcal{L}$	0.0002	-0.006	0.017	-0.007	

TABLE I. Estimates of the critical energies and latent heat for PM-10 using raw data set RS.

L	30	40	50	60	Exact
e_o	-1.665(17)	-1.669(21)	-1.666(3)	-1.666(7)	-1.66425...
$\frac{\Delta e_o}{\sigma_o}$	0.0	0.2	0.6	0.2	
e_d	-0.983(5)	-0.992(9)	-0.962(2)	-0.969(3)	-0.96820...
$\frac{\Delta e_d}{\sigma_d}$	3.0	2.6	3.1	0.3	
\mathcal{L}	0.682(22)	0.677(30)	0.704(5)	0.697(10)	0.696049...
$\Delta\mathcal{L}$	-0.014	-0.019	0.008	0.001	

TABLE II. Estimates of the critical energies and latent heat for PM-10 using majority/minority data set MS.

Tables III and IV present estimates of critical energies e_o and e_d and latent heat for the 20-component Potts model, PM-20. The quality of estimates is as good as those in the case of the PM-10 model. Again, our data show no noticeable dependence of the estimates on the system size. In this case, the correlation length in the critical point is much smaller at about 2.7 [24], and yet we see no finite-size corrections in our estimates. In contrast, in our recent study on PM-10 and PM-20 [19] using the Wang-Landau algorithm in simulations and the same MCPA algorithm as in the present research, the finite-size corrections to the critical energies estimated from the energy probability distribution show $1/L$ corrections, as predicted by the analytics [25, 26].

Discussion. — In contrast to binary classification in the case of a phase transition of the second kind, our approach is based on ternary classification, using for training exactly known energies of the ordered phase e_o and disordered phase e_d . To do this, we need to train the neural network on samples modeled at a certain value of energy e . For this purpose, we use the microcanonical population annealing algorithm (MCPA) [16, 17, 19], which anneals a large population of the modeled system in energy space. The trained network is used to classify

L	30	40	50	60	Exact
e_o	-1.820(12)	-1.821(11)	-1.813(2)	-1.821(15)	-1.82068...
$\frac{\Delta e_o}{\sigma_o}$	0.1	0.0	3.8	0.0	
e_d	-0.616(3)	-0.652(6)	-0.606(26)	-0.638(3)	-0.626529...
$\frac{\Delta e_d}{\sigma_d}$	3.5	4.2	0.8	3.8	
\mathcal{L}	1.204(15)	1.169(17)	1.207(28)	1.183(18)	1.19415...
$\Delta\mathcal{L}$	0.010	-0.025	0.013	-0.011	

TABLE III. Estimates of the critical energies and latent heat for PM-20 using raw data set RS.

L	30	40	50	60	Exact
e_o	-1.818(2)	-1.824(17)	-1.821(31)	-1.819(8)	-1.82068...
$\frac{\Delta e_o}{\sigma_o}$	1.3	0.2	0.0	0.2	
e_d	-0.632(1)	-0.638(12)	-0.657(7)	-0.636(3)	-0.626529...
$\frac{\Delta e_d}{\sigma_d}$	5.5	1.0	4.4	3.2	
\mathcal{L}	1.186(3)	1.186(29)	1.164(38)	1.183(11)	1.19415...
$\Delta\mathcal{L}$	-0.008	-0.008	-0.030	-0.011	

TABLE IV. Estimates of the critical energies and latent heat for PM-20 majority/minority data set MS.

all samples taken at a given energy e into those that are more likely to be in ordered, disordered, or mixed phase. Thus, we can estimate the probability that a given sample belongs to one of the three phases. This protocol allows us to estimate critical energies and latent heat with reasonable accuracy.

At the same time, we found that the estimated probabilities contain some information about the details of the mixed phase. It is widely believed that there are four

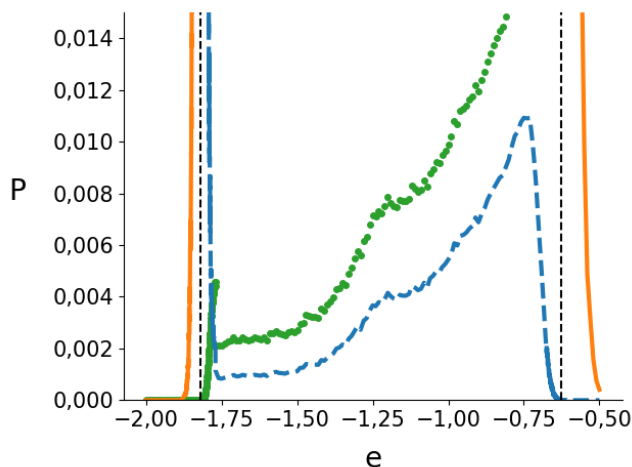


FIG. 5. Enlarged details of the left panel of the figure 4 showing small probability values with some features discussed in the Discussion section. Potts model with 20 components, PM-20 with grid size $L = 60$.

phase transitions in the mixed phase, which is a random mixture of ordered and disordered phases [14, 16]. In the case of the Potts model, these are droplets that reflect the ordered and disordered phases [27].

In the figure 5, the solid orange line corresponds to the mixed phase probability P_{MS} , the dotted green line corresponds to the disordered phase probability P_{DS} , and the dashed blue line corresponds to the ordered phase probability P_{OS} . The rightmost peak of P_{OS} can be associated with the transition at energy $e_1(L)$ using the notations of Rose and Machta [16]. It is associated with the fluctuating droplets of OS phase within the DS sea, which vanishes at e_d . It is the precursor of the phase transition from mixed phase MS to disordered phase DS, as $e_1(L) \rightarrow e_d$ in the thermodynamic limit. By analogy, the leftmost peak of P_{OD} can be associated with the transition at energy $e_4(L)$ and reflects DS droplets within the emerging sea of OS phase. Again, $e_4(L) \rightarrow e_o$ and the DS droplets completely vanishes at e_o . So, the transitions at $e_1(L)$ and $e_4(L)$ can be obtained only in the systems of finite size, and are not real phase transitions.

More interesting is the presence of small extrema on the DS and OS curves in the middle of the mixed phase. They can be related to the wrapping clusters when DS or OS droplets reach opposite boundaries of the system and due to the periodic boundaries will “wrap” around the torus. It is argued [14, 16, 27] that the transitions at e_2 and $e_3 < e_2$ associated with the wrapping droplet OS and wrapping droplet DS, respectively, exist in the thermodynamic limit. Note that the extrema shown in our figure 5 are qualitatively similar to the extrema of a very different function, the integrated autocorrelation time shown in the Fig. 5 of the article [16].

It would be interesting to apply the phase probability estimation method proposed in the Letter to a regular analysis of the above pattern. With a possible demonstration of regular limits of $e_1(L)$ and $e_4(L)$ with increasing L , and also a clear idea of droplet \leftrightarrow wrapping cluster transitions.

The simulation was carried out using the high-performance computing resources of the National Research University Higher School of Economics.

The research was supported by the Russian Science Foundation Grant No. 22-11-00259.

-
- [1] Sen, P.C., Hajra, M., Ghosh, M. (2020). Supervised Classification Algorithms in Machine Learning: A Survey and Review. In: Mandal, J., Bhattacharya, D. (eds) Emerging Technology in Modelling and Graphics. Advances in Intelligent Systems and Computing, vol 937. Springer, Singapore. https://doi.org/10.1007/978-981-13-7403-6_11
- [2] G. Carleo, I. Cirac, K. Cranmer, L. Daudet, et al., *Ma-*

- chine learning and the physical sciences*, Rev. Mod. Phys. **91**, 045002 (2019).
- [3] J. Carrasquilla and R.G. Melko, *Machine learning phases of matter*, Nat. Phys. **13**, 431 (2017).
- [4] V. Chertentkov, E. Burovski, and L. Shchur, *Finite-size analysis in neural network classification of critical phenomena*, Phys. Rev. E **108**, L031102 (2023).
- [5] J. Zhang, B. Zhang, J. Xu, W. Zhang, and Y. Deng, *Machine learning for percolation utilizing auxiliary Ising variables*, Phys. Rev. E **105**, 024144 (2022).
- [6] Bachtis, D., Aarts, G., Lucini, B.: Mapping distinct phase transitions to a neural network. Phys. Rev. E **102**(5), 053306 (2020).
- [7] Van Nieuwenburg, E.P., Liu, Y.H., Huber, S.D.: Learning phase transitions by confusion. Nat. Phys. **13**, 435 (2017).
- [8] Morningstar, A., Melko, R.G.: Deep learning the Ising model near criticality. J. Mach. Learn. Res. **18**, 1 (2018).
- [9] Westerhout, T., et al.: Generalization properties of neural network approximations to frustrated magnet ground states. Nat. Commun. **11**, 1593 (2020).
- [10] Miyajima, Y., Mochizuki, M.: Machine-Learning Detection of the Berezinskii-Kosterlitz-Thouless Transition and the Second-Order Phase Transition in the XXZ models. Phys. Rev. B **107**, 134420 (2023).
- [11] D.D. Sukhoverkhova and L.N. Shchur, *Influence of anisotropy on the study of critical behavior of spin models by machine learning methods*, Pis'ma v ZhETF, **120**, 644 (2024) in Russian and arXiv:2410.14523 - English translation.
- [12] V. Chertentkov and L. Shchur, *Machine Learning Domain Adaptation in Spin Models with Continuous Phase Transitions*, submitted to PRL.
- [13] Since the critical values of e_o and e_d are irrational and the energies have rational values on a finite size lattice, exact equalities are not achieved by numerical investigation.
- [14] T. Neuhaus and J.S. Hager, *2D Crystal Shapes, Droplet Condensation, and Exponential Slowing Down in Simulations of First-Order Phase Transitions*, J. Stat. Phys. **113**, 47 (2003).
- [15] V. Martin-Mayor, *Microcanonical Approach to the Simulation of First-Order Phase Transitions*, Phys. Rev. Lett. **98**, 137207 (2007).
- [16] N. Rose and J. Machta, *Equilibrium microcanonical annealing for first-order phase transitions*, Phys. Rev. E **100**, 063304 (2019).
- [17] V.K. Mozolenko, and L.N. Shchur, *Blume-Capel model analysis with a microcanonical population annealing method*, Phys. Rev. E **109**, 045306 (2024).
- [18] R.B. Potts, *Some generalized order-disorder transformations*, Proc. Cambridge Philos. Soc. **48**, 106 (1952).
- [19] V.K. Mozolenko, M.A. Fadeeva, and L.N. Shchur, *Comparison of the microcanonical population annealing algorithm with the Wang-Landau algorithm*, Phys. Rev. E **110**, 045301 (2024).
- [20] K. Binder, *Static and dynamic critical phenomena of the two-dimensional q-state Potts model*, J. Stat. Phys. **24**, 69 (1981).
- [21] K. O'Shea and R. Nash, *An introduction to convolutional neural networks*, <https://arxiv.org/abs/1511.08458>.
- [22] Kingma D., Ba J.: Adam: A Method for Stochastic Optimization, arXiv:1412.6980
- [23] D. Sukhoverkhova, V. Chertentkov, E. Burovski, and L. Shchur, *Validity and Limitations of Supervised Learning for Phase Transition Research*, in Supercomputing, V. Voevodin et al. (Eds.): RuSCDays 2022, LNCS **13708**, 397 (2022).
- [24] C. Borgs and W. Janke, *An explicit formula for the interface tension of the 2D Potts model*, J. Phys. I France **2**, 2011 (1992).
- [25] M.S.S. Challa, D.P. Landau, and K. Binder, *Finite-size effects at temperature-driven first-order transition*, Phys. Rev. B **34**, 1841 (1986).
- [26] J. Lee and J.M. Kosterlitz, *Finite-size scaling and Monte Carlo simulations of first-order phase transitions*, Phys. Rev. B **43**, 3265 (1991).
- [27] K. Leung and R. K. P. Zia, *Geometrically induced transitions between equilibrium crystal shapes*, J. Phys. A: Math. Gen. **23**, 4593 (1990).